Journal of Power Sources 200 (2012) 21–28

Contents lists available at SciVerse ScienceDirect

Journal of Power Sources

journal homepage: www.elsevier.com/locate/jpowsour

Strategy to optimize cathode operating conditions to improve the durability of a Direct Methanol Fuel Cell

Charn-Ying Chen, Hou-Chin Cha*

Institute of Nuclear Energy Research (INER), 1000, Wenhua Rd., Chiaan Village, P.O. Box 3-14, Lungtan, Taiwan

ARTICLE INFO

Article history:
Received 21 September 2011
Received in revised form 28 October 2011
Accepted 31 October 2011
Available online 4 November 2011

Keywords:
Direct Methanol Fuel Cell
Membrane electrode assembly
Cathode operating conditions
Polarization curve
Electrochemical Impedance Spectroscopy

ABSTRACT

This study addresses optimal cathode operating conditions to improve the durability of Direct Methanol Fuel Cells (DMFCs). Usually, CO-like adsorbents may poison Pt catalysts and flooding may lead to starvation of the reactant or hindrance of mass-diffusion. Both of these conditions can greatly decrease cell performance; thus, modified operating conditions are needed to lessen the disadvantages. By means of the proposed strategies, including an air on/off condition during the load-off mode, a load on/off interval and an air flow rate during the load-on mode, the degradation rate can be successfully restrained. Resistance *R* obtained by the individual polarization curve is essential for identifying the main component affecting cell performance. By incorporating Electrochemical Impedance Spectroscopy (EIS), the degradation mechanism can be characterized. The electrochemical surface area (ECA) is employed to investigate the actual chemical degradation, unlike the results in most other reports; the loss in the anode catalyst is discovered to be the main detriment, which is attributed to our modified cathode operating conditions. Notably, a thin metal oxide is found on the surface of the test block after long-term operation, and its influence is also assessed to clarify the actual performance loss of the MEA (membrane electrode assembly).

1. Introduction

In recent decades Direct Methanol Fuel Cells (DMFCs) have shown great promise due to their high energy density, compact system, ease of operation and instantaneously rechargeable power source for portable electronic devices [1–3]. However, some of the issues, such as sluggish oxidation reaction on the anode side and loss of hydrophobic degree at the cathode side are, in fact, hindering the commercialization of a DMFC. The anodic reaction in a DMFC is imperfect because methanol is decomposed into CO, with formaldehyde and formic acid as its principal by-products which are corrosive to the membrane electrode assembly (MEA) [4–7]. Water management is of great importance to ensure stable operation and high efficiency of DMFC in a long-term test. The loss of the degree of hydrophobicity in the catalyst and diffusion layers will allow the channels to accumulate too much water; this causes reactant starvation and eventually negatively impacts the performance and lifetime of a DMFC [7–9]. The degradation mechanisms for each of the individual components that comprise DMFCs must be well characterized to improve their durability.

Fig. 1(a) shows the long-term durability test in our previous work [7]. When the MEA was in good health (before 1200 h), the cell voltage maintained a high performance but decreased slightly with time. The cell voltage decreased with time but could be partially recovered after every interruption caused by the stop/restart procedure. The stop/restart procedure, which came after a 24-h continuous constant-load operation, maintained the methanol solution circulation but cut off the air supply without electric load for 1–2 min. Then, the procedure turned on the electric load while the air was being resupplied. The periodic on/off switching of the applied load seemed to be effective in recovering performance loss that occurred during fuel cell operation. However, after 1200 h, the MEAs degraded dramatically, and the cell voltage experienced unrecoverable performance loss. Fig. 1(b) shows the abnormal cell voltage profile after an operation time of 1200 h. For Sample A, the cell voltage rebounded to a higher value after the stop/restart procedure; however, the degradation rate of Sample A quickened, and the cell voltage was even lower than before. For Sample B, the situation was much worse. The cell voltage could not rebound to a higher value after the stop/restart procedure, but began with a negative cell voltage and then crept up slowly to the positive side. Both conditions affecting Samples A and B could be alleviated temporarily by keeping the load-off mode for a longer period or supplying a huge air impulse on the cathode side. Thus, the dramatic performance loss after an operation time of 1200 h could be attributed to the inactivity of the catalyst and the flooding phenomenon in the catalyst layer (CL) and gas diffusion layer (GDL). On the anode side, some unexpected species strongly adsorbed on

* Corresponding author. Tel.: +886 3 4711400x2960; fax: +886 3 4711409.
E-mail address: hccha@iner.gov.tw (H.-C. Cha).

0378-7753/$ – see front matter © 2011 Elsevier B.V. All rights reserved.
doi:10.1016/j.jpowsour.2011.10.100

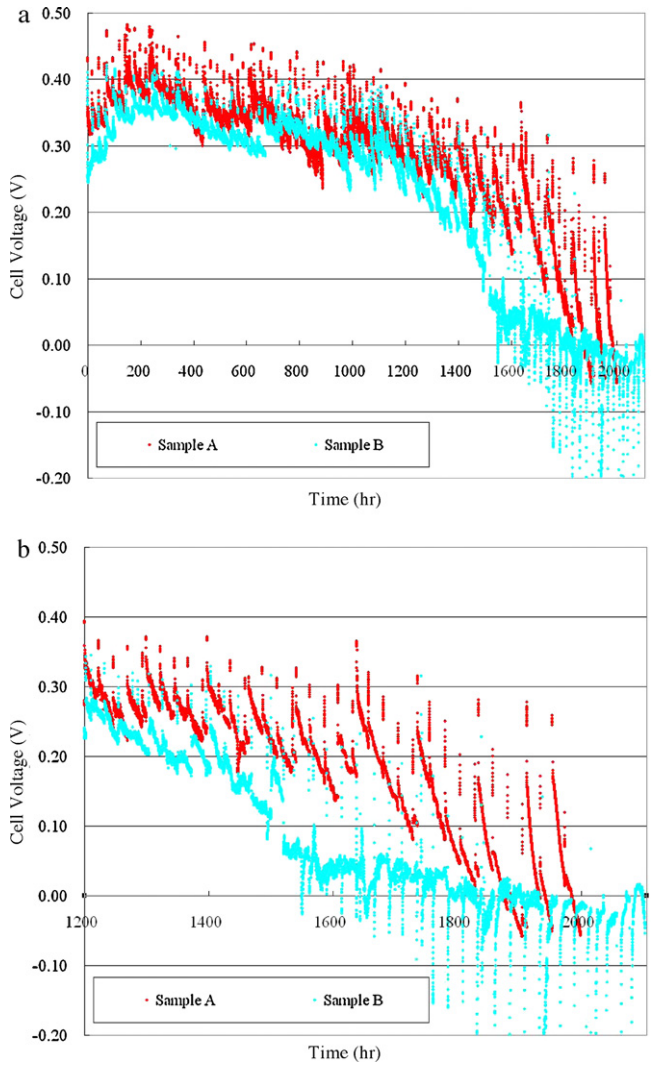

Fig. 1. Durability test of DMFC. Operating condition: cell temperature at 70 °C, 100 mA cm^{-2} (3 A). Anode feed: 2.2 wt.% CH_3OH, flow rate 20 ml min^{-1}. Cathode feed: air, flow rate 0.5–1 L min^{-1}. (a) Entire period and (b) zoom-in after 1200 h.

the catalyst surface, preventing adsorption and further reaction of fresh methanol, would facilitate some degradation mechanisms [4]. Besides, once the water accumulated in the catalyst layer or gas diffusion layer at the cathode while operating, the performance would degrade gradually as the effective reaction area decreased. Moreover, the degree of hydrophobicity of the components in DMFC would be destroyed and water would permanently occupy the cathode's side. Finally, the performance loss could no longer be saved. Thus, some strategies should be designed to maintain the cell performance and thus prolong the DMFC life span.

Electrochemical Impedance Spectroscopy (EIS) has long been utilized to probe interfacial processes and speciation in electrochemical systems. EIS reveals characteristics such as high-frequency resistance (HFR) and charge-transfer resistance (CTR), which can be used to inspect the resistance of the membrane, electrodes and contacts, or examine the mass transportation capability of the MEA. EIS studies of DMFCs under various test conditions, such as a large electrode area, high temperature, freezing cycles and a large DC current, have recently been performed [10–18]. The electrochemical surface area (ECA) loss estimates the real loss of cell performance owing not only to the change in the microstructure, such as agglomeration and growth of catalysts, but also to the poisoning of the catalysts by intermediates and impurities after a durability test. In this work, several test strategies are carried out to optimize the cell performance for mitigating the degradation, including the air on/off condition during the load-off mode, the load on/off interval and the air flow rate during the load-on mode. In order to obtain a better understanding of the correlation between the degradation mechanism and DMFC performance, electrochemical analyses are implemented. By incorporating the ECA measurements with EIS results, performance loss due to catalyst inactivity or poor resistance due to contact or diffusion can be easily judged.

2. Experimental

2.1. MEA preparation and fabrication

The MEA was a commercial product made of Nafion 117 membrane with a five layer structure (GDL/CL/membrane/CL/GDL). Catalysts of the MEA on the anode and cathode sides were Pt:Ru (1:1 atomic ratio) and Pt, respectively, and the catalyst loading was 2 mg cm^{-2} on each side. The material used for GDLs on both the anode and cathode sides was carbon paper; an unknown amount of catalyst was discovered in the micro-porous layer (MPL) on the anode side. The active areas of all MEAs were 25 cm^2, and the gasket thickness of the anode and cathode sides were 0.2 and 0.15 mm, respectively. The MEA was installed in a test block which made of stainless steel-plated (Type 316). A serpentine–serpentine flow field was machined in the plates with parallel geometry (1 mm wide, 1.2 mm deep, with ridges 1 mm high).

2.2. Single-cell operation

A thermocouple was used to monitor and control the desired cell temperature. A 3 wt.% methanol solution was fed from a methanol container with a pump and preheated to the operating temperature. The flow meter was positioned after the compressor valve to regulate the air flow at room temperature. Before the EIS measurement, the cell was preheated to 70 °C for 1 h without an air supply. The current–voltage (polarization curves) and current–power characteristics were measured galvanostatically with an electronic loader (Prodigit 3300C).

2.3. Characterization of MEA

The impedance spectra and the ECA results were recorded with a ZAHNER IM 6ex instrument. To resolve the anode and cathode impedance, an Ag/AgCl electrode (MF-2052, BAS Inc.) was placed in the membrane's region of constant potential (RCP) [19–21] as a reference electrode. For measurement of the half-cell impedance of the anode, the cathode electrode was operated as a dynamic hydrogen electrode (DHE). Clearly, the real HFR of the anode can be isolated by using Ag/AgCl. Furthermore, the CTR of each electrode, as well as the individual HFR, was separated during operation of the different airflows at 100 and 300 ml min^{-1}. The range of measured frequencies was set from 1 kHz to 0.1 Hz with 10 steps per logarithmic decade. The detailed description of the setup of the reference electrode was proposed and demonstrated in our previous work [19]. All of the impedance spectra were measured under the galvanostatic mode. The catalysts' ECAs were evaluated by hydrogen-desorption. A reaction of interest was the electrochemical reduction of protons (H^+) and subsequent deposition of atomic hydrogen on the surface of the Pt catalyst, $Pt + H^+ + e^- \leftrightarrow Pt–H_{ads}$. The atomic hydrogen adsorption charge density, due to this reaction, could be determined from the CV scan. For the anodic ECA test, the cathode serving as a DHE was fed humidified hydrogen at 20 ml min^{-1}. The anode was fed with humidified nitrogen at 300 ml min^{-1}. On the contrary, for the cathodic ECA test, the anode

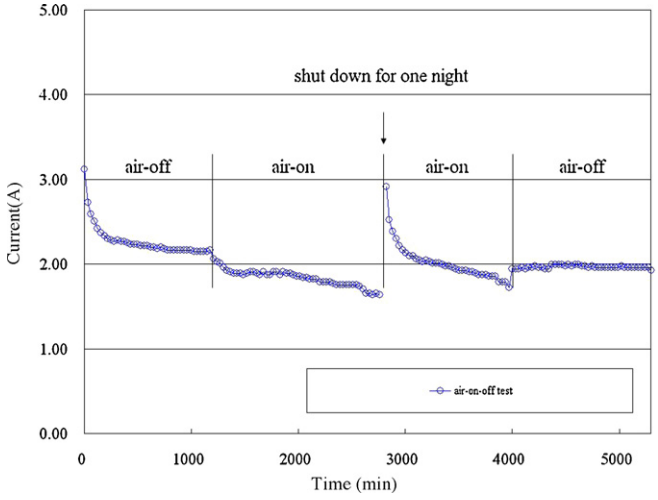

Fig. 2. Air-on-off test during the load-off mode. Cell temperature is 70 °C, both the anode and cathode flow are 6-stoichiometry at a constant voltage of 425 mV. Anode feed: 3 wt.% CH_3OH. Cathode feed: air. The load-on-off interval is 30 min-on 2 min-off.

serving as a DHE was fed with humidified hydrogen at 20 ml min^{-1}. The cathode was fed with humidified nitrogen at 300 ml min^{-1}. The potential was then scanned from 0 to 0.8 V at a scan rate of 20 mV s^{-1} on both the anode and cathode side. The ECA of the Pt catalyst [22] was calculated from the charge density, the well-established quantity for the charge to reduce a monolayer of protons on Pt.

3. Results and discussion

3.1. Optimal operating conditions

The performance degradation of a DMFC appears to be a gradual process, the extent of which depends on time as well as operating conditions. The overall degradation in cell performance may stem from both temporary losses and permanent failure in the system's components. The DMFC performance degradation, which originates from temporary losses, can be recovered either partially or fully. Park et al. proposed a load on/off recovery technique which was tested by periodically removing the electric load from the cell for 30 s followed by normal operation for 30 min (30 s off and 30 min on). During the load-off mode, other conditions like cell temperature, pressure and reactants' flow rates were maintained the same as those for the load-on conditions [23]. The reduced decay rate in 200 h was found to be 0.47 mV h^{-1} @ 100 mA cm^{-2}, which was better than that of the continuous constant load (0.80 mV h^{-1}). However, some operating conditions still could be regulated to improve the performance and durability of a DMFC as described in the following:

(1) Air on/off condition during load-off mode

Obviously, air is a key factor for optimizing cell performance, and Fig. 2 shows the impact of the air conditions on cell performance. The air flow rate, corresponding to cathode stoichiometry of 6, was set at a constant voltage of 425 mV. The stoichiometric flow rate of the anode was also set at 6 when a 3 wt.% methanol solution was used at 70 °C. The load on/off condition was set at 30 min on and 2 min off, and the air on/off conditions were carried out to obtain the optimal cell performance during the load-off mode. The cell currents were recorded after supplying the load for 1 min during each load-on mode. It was noted that, in order to prevent the MEA from experiencing air starvation at the start of load-on mode, 15 s of air was supplied into the cathode before the load-on condition in all experiments. During the first air-off mode, the cell current decreased quickly for the first 300 min and degraded slowly until 1200 min. The remarkable performance loss during the first 300 min might be attributed to the accumulation of CO_2 bubbles, by-products and water on the surface of the MEA due to an oxidation-reduction reaction (ORR) of the fresh catalysts. Since the products accumulated in the catalyst layer did not balance, the degradation rate increased gradually. Once the products of the ORR were saturated, the degradation rate was suppressed. However, when the air on/off condition was switched from air-off to air-on, the cell current dropped suddenly. The experiment paused overnight at the time of 2800 min and then restarted from the air-on during load-off mode. Undoubtedly, the cell current exhibited a performance increment when the air on/off condition was switched from air-on to air-off. Despite the operating sequence of air on/off condition, the cell always exhibited superior performance under air-off during load-off mode.

The increase in performance was probably related to efficient removal of water in the cathode by the air on/off process; it could also be reasonably explained by the depoisoning of the electrode surface through oxidation of the CO-like adsorbents. The depoisoning produced more free surface sites for the methanol oxidation reaction (MOR). Hence, the air-off

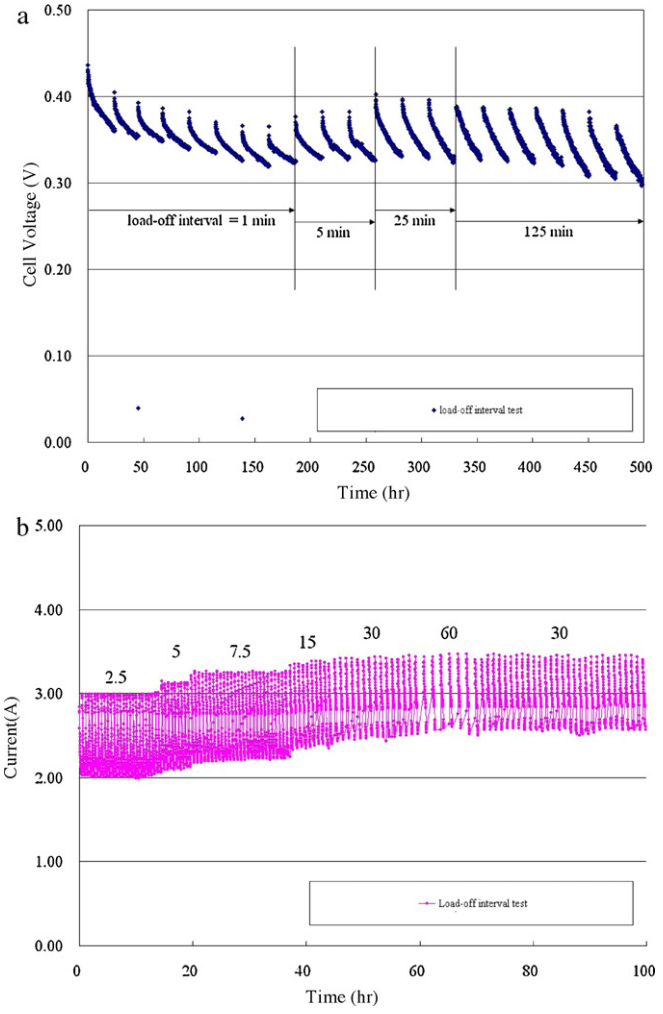

Fig. 3. Load-on-off interval test. Cell temperature is 70 °C, both the anode and cathode flow are 6-stoichiometry. Anode feed: 3 wt.% CH_3OH. Cathode feed: air. (a) Constant current of 160 mV cm^{-2} and (b) constant voltage of 425 mV.

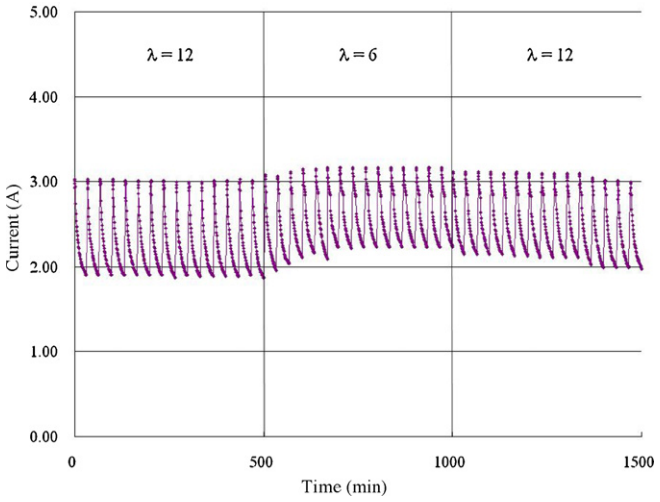

Fig. 4. Air flow rate test during the load-on mode. Cell temperature is 70 °C, both the anode and cathode flow are 6-stoichiometry at a constant voltage of 425 mV. Anode feed: 3 wt.% CH_3OH. Cathode feed: air. The load-on-off interval is 30 min-on 2 min-off.

condition during the load-off mode appeared to be effective in increasing the active sites of the catalyst. These phenomena originated from the cell voltage behavior during the load-off mode. According to previous reports [24,25], at high positive potentials a Pt oxide layer formed due to the oxidation of Pt itself, or corrosion of the carbon support occurred and it decreased the number of Pt active sites. Besides, a low potential at the cathode (below 0.5 V versus RHE) could reduce the surface oxide of the Pt catalyst and rapidly consume oxygen at the cathode, thereby leading to possible recovery of the performance of the DMFC cathode [26]. Therefore, the voltage drop at the cathode side under the load-off state appears to promote depoisoning of the catalyst surface as well as better performance of the cell under the air-off condition during the load-off mode.

(2) Load on/off interval

Load-on and load-off mode intervals are another issue for restoring performance loss. Fig. 3 shows the different load on/off intervals for recognizing the performance change of a DMFC. In Fig. 3(a), the air flow rate, corresponding to the cathode stoichiometry of 6, was set at a constant current of 160 mA cm^{-2}. The stoichiometric flow rate of the anode was set at 6 when a 3 wt.% methanol solution was used at 70 °C. The load-on interval of each cycle was 24 h and the load-off interval (air-off condition) was sequentially tested for 1, 5, 25 and 125 min. When the load-off interval was set at 1 min, the cell performance degraded gradually and the peak voltage could not rebound to that of the last cycle. As the load-off interval increased, the performance loss began to recover and the maximum increment was reached when the load-off interval was set at 25 min. It was noted that the peak voltage of the 125 min load-off interval showed a slight decrement, which might result from the lower temperature due to a longer period without chemical reaction. In Fig. 3(b), reactant flow, temperature and methanol concentration were all the same as Fig. 3(a), but the load-on condition was set at a constant voltage of 425 mV. The load-on interval for each cycle was 30 min and the load-off interval (air-off condition) were sequentially tested for 2.5, 5, 7.5, 15, 30 and 60 min. Like the results shown in Fig. 3(a), the cell performance gradually increased as the load-off interval was prolonged, and the peak current showed no further increment when the load-off interval was above 30 min. It could

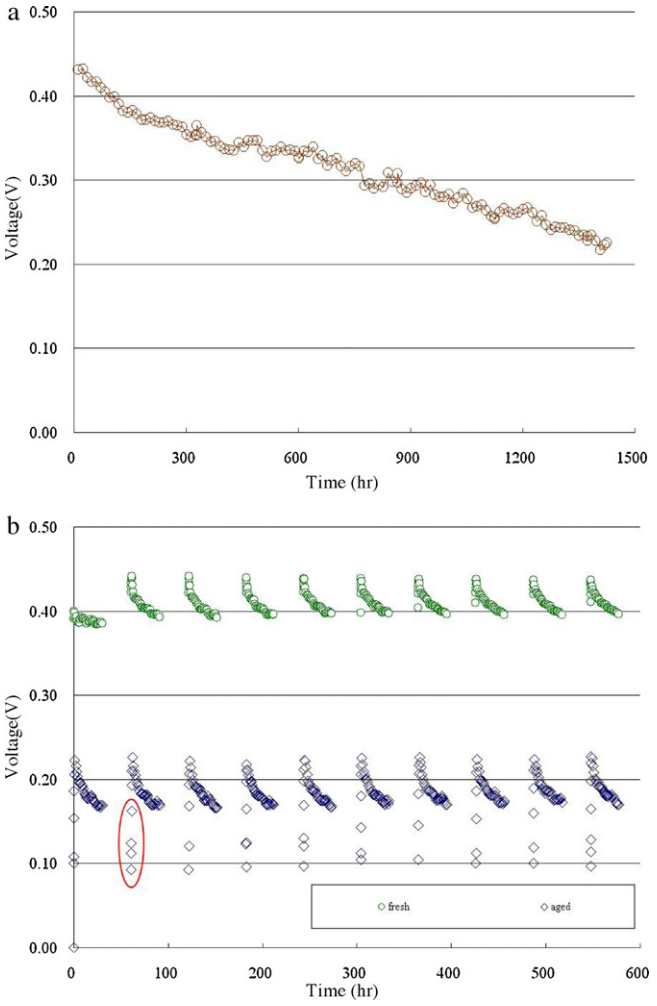

Fig. 5. Durability test of DMFC. Operating condition: cell temperature at 70 °C, both the anode and cathode flow are 6-stoichiometry at a constant current of 200 mA cm^{-2} (5 A). Anode feed: 3 wt.% CH_3OH. Cathode feed: air. (a) Degradation rate versus time and (b) performance of the fresh and aged MEA.

be concluded that longer load-off intervals exhibit superior restoration of the DMFC performance, and the optimal load-off interval is about 30 min in both cases. Thus, a low potential at the cathode side was the necessary factor to recover cell performance; furthermore, with the addition of the proper load-off interval, the maximum peak performance could be reached.

Regarding the load-on interval, the degradation rates for each cycle (24 h) shown in Fig. 3(a) increased gradually with time from 1.66 mV h^{-1} (at 24 h) to 3.26 mV h^{-1} (at 450 h). Hence, long-term operation was disadvantageous for removing excess water and would induce a degradation mechanism due to air-starvation. Moreover, the Pt oxide layer was consecutively adsorbed on the surface of the catalyst, and that would eventually hinder the ORR of the cathode catalyst. Without strategies for alleviating the degradation rate, the performance loss accelerated and could not be recovered. However, as seen in Fig. 3(b), the experiment proceeded to 600 h (data not shown), and the degradation rate remained almost unaltered at each cycle. The load on/off interval was of importance as a key parameter for improving the durability of a DMFC, and the optimal combination was 30 min on and 30 min off without an air-supply during the load-off mode.

(3) Air flow rate during load-on mode

Generally, flooding was caused by excess water on the cathode side, and the situation got worse for aged MEA. Considering

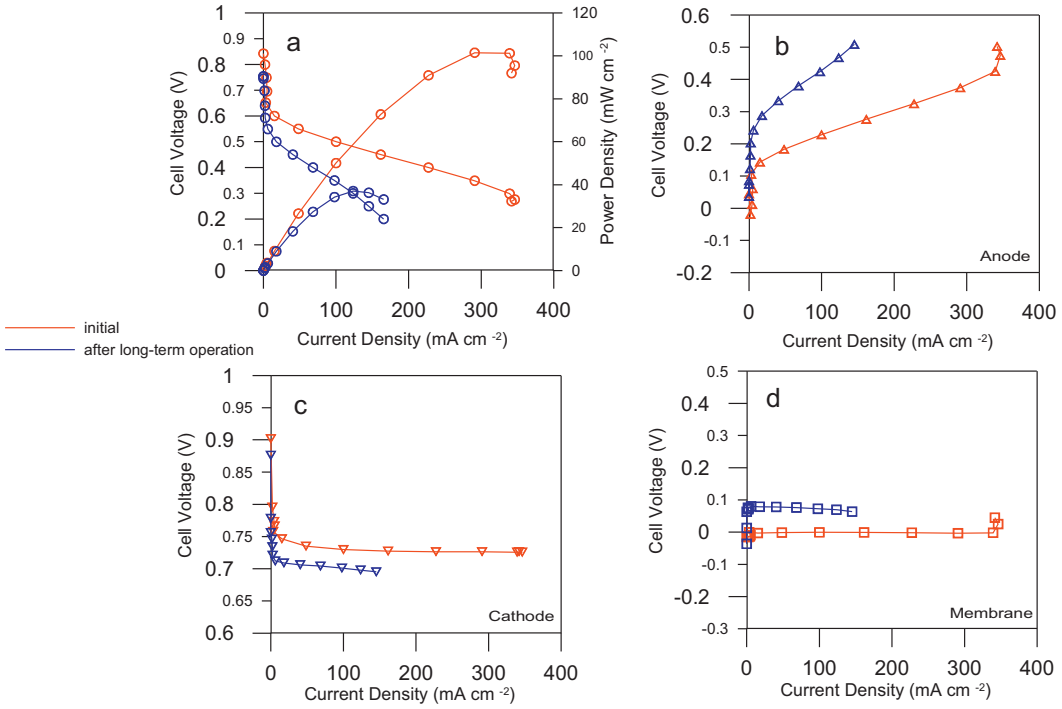

Fig. 6. Polarization curves of the MEA during the long-term operation: (a) full-cell, (b) anode, (c) cathode, and (d) membrane. Cell temperature is 70 °C, both the anode and cathode flow are 6-stoichiometry.

the water removal on the cathode side, an elevated air flow rate was used to verify the impact on cell performance. Fig. 4 shows that the different air flow rates, corresponding to cathode stoichiometry of 6 and 12, were set at a constant voltage of 425 mV. The stoichiometric flow rate of the anode was set at 6 when a 3 wt.% methanol solution was used at 70 °C, and the load on/off condition was set at 30 min on and 2 min off (air-off). At first, an elevated air flow rate ($\lambda = 12$) was supplied to the cathode side for 500 min, and the cell performance was kept stable without obvious degradation. After that, the air flow rate was

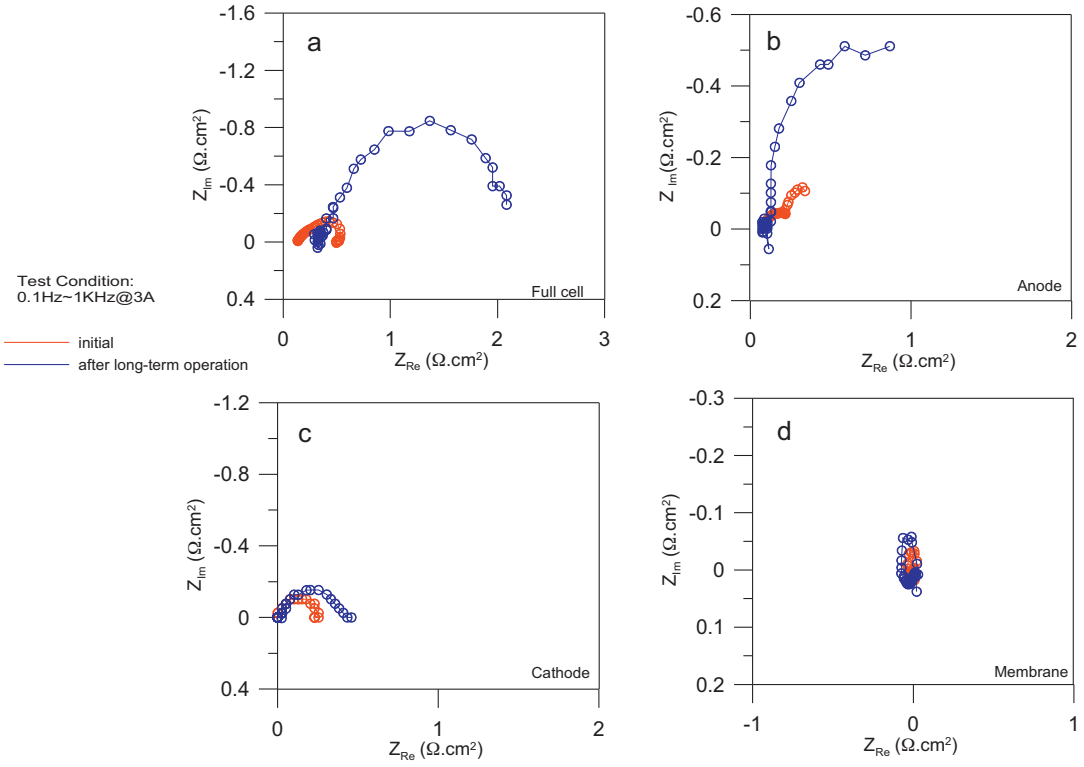

Fig. 7. EIS measurement results of the MEA during the long-term operation: (a) full-cell, (b) anode, (c) cathode, and (d) membrane. Cell temperature is 70 °C, both the anode and cathode flow are 6-stoichiometry.

switched from λ = 12 to λ = 6, and the peak current increased gradually by about 5.11% in 120 min. However, after 1000 min, the air flow rate was switched back to λ = 12, and the cell performance degraded again. When the air flow rate was switched from λ = 6 to λ = 12, the cell performance could be kept for a short period, but it dropped with time as the MEA underwent another hindrance. Theoretically, an elevated air flow rate of λ = 12 could keep the cell performance the same as that of the air flow rate of λ = 6; nevertheless, with long-term operation, the membrane would be too dry to restrain the conductivity of the proton. Although an elevated air flow rate has a superior ability to remove water, the degraded performance due to inferior proton diffusion would eventually erase the inherent benefit. On the other side, when the air flow rate was switched from λ = 12 to λ = 6, the cell performance recovered as the proton conductivity of the membrane increased. It could be concluded that with the moderate air flow rate (λ = 6), the cell revealed better performance while the condition on the cathode side was favorable for both water removal and proton diffusion.

3.2. Long-term durability test

Strategies to optimize the cathode conditions for improving performance were carried out and the improved results of a long-term durability test are shown in Fig. 5(a). The air flow rate, using a constant voltage of 200 mA cm^{-2}, was set at λ = 6. The stoichiometric flow rate of the anode was set at 6 with a 3 wt.% methanol solution at 70 °C. The load on/off condition was set at 30 min on and 30 min off with the air-off during the load-off mode. The cell voltages were recorded after supplying the load for 1 min during each load-on mode. In comparison with the previous report [23], the degradation rate of the improved strategies in the first 200 h was only 0.28 mV h^{-1}, which was superior even at a higher current density of 200 mA cm^{-2}. The degradation rate of the entire long-term process (1450 h) was further improved to be 0.145 mV h^{-1}. In comparing the beginning and the end of the load-on performance in the durability test, the first 600 min (fresh) and the last 600 min (aged), shown in Fig. 5(b), were taken into consideration. The cell performance dropped about 50% after long-term operation, however, the degradation rate at each cycle seemed almost unaltered and the peak voltage was almost the same as that of the last cycle, which implies that the strategies for optimizing the cathode condition successfully removed the excess water and desorbed the Pt oxide layer, thereby preserving the cell performance at an adjacent operation period. However, the cell voltage at the start of the load-on mode exhibited delayed response for the aged MEA (as indicated by the red circle) which may result from the diffusion problem of reactants or products due to chemical reaction. Thus, further measurements of EIS and ECA were employed to understand the degradation mechanism.

3.3. EIS and ECA results

Fig. 6 shows the polarization curves associated with the individual anode, cathode and membrane performance of the MEA. Fig. 6(a) shows that the MEA, after a 1450 h test from Fig. 5, performed worse than the fresh MEA. Peak performance loss was estimated to be about 60%. Fig. 6(b) shows the individual anode polarization curve. The increased $|\Delta V/\Delta I|$ values corresponding to the resistance R might have resulted from microstructural changes damaging the catalyst layer and delaminating the GDL. Fig. 6(c) and (d) shows the individual cathode and individual membrane polarization curves, respectively. Both the $|\Delta V/\Delta I|$ values were almost the same after long-term operation, which implies that the cathode and the membrane were not the main determinant

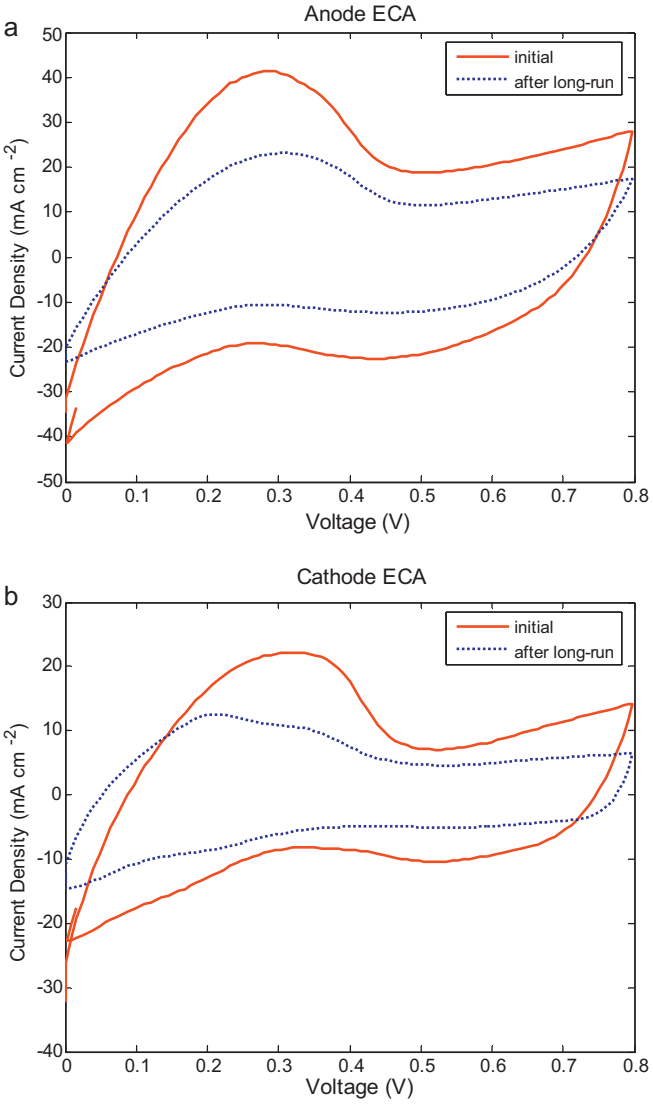

Fig. 8. Electrochemical areas (ECAs) of the catalysts on MEA evaluated by hydrogen-desorption test: (a) anode catalysts and (b) cathode catalysts.

of the polarization curve. Thus, the major performance loss could be attributed to the degradation on the anode side.

Fig. 7 shows the electrochemical behavior of the MEA. Fig. 7(a) plots a full-cell impedance spectrum. The HFR corresponding to the ohmic resistance of cell elements was the sum of the resistances, such as the membrane, electrodes, contacts, and other components. Since the HFR of the full-cell impedance spectrum increased, a long-term durability test might negatively affect the contact resistance. This mechanism will be discussed later. In the initial state, the CTR of the full-cell spectrum showed a small arc when the MEA was in a normal condition. After 1450 h test from Fig. 5, the diameter of the arc increased and the arc diverged in the low-frequency region. The causes of this change in the CTR spectra were revealed by the individual anode, cathode and membrane impedance spectra. Fig. 7(b) presents the CTR spectrum of an individual anode. The double arcs

Table 1
Electrochemical surface area of different operation periods.

	Anode (m^2 g^{-1})	Cathode (m^2 g^{-1})
Initial	88.394	44.162
After long run	47.64	26.558
After polishing	54.817	32.864

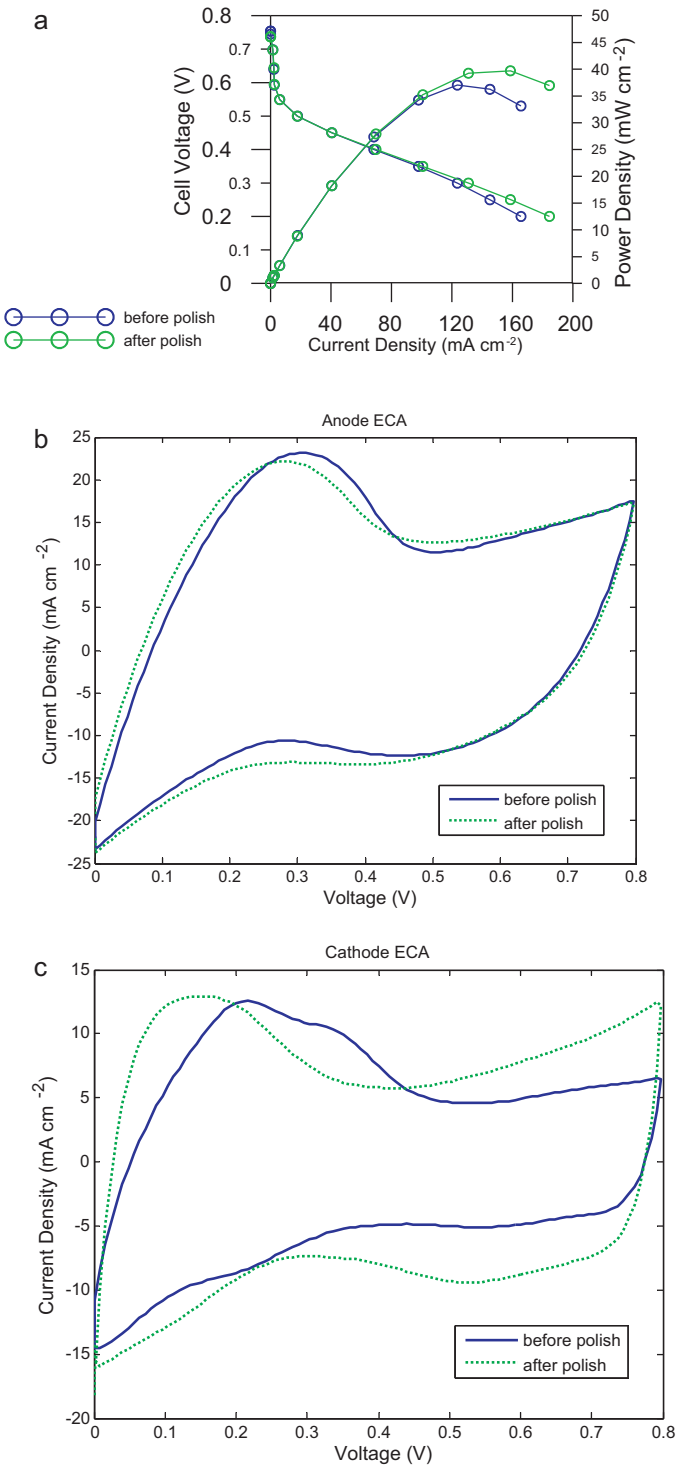

Fig. 9. Characteristics of the MEA after polishing the metal oxide on the surface of the test block: (a) polarization curves, (b) anode catalysts, and (c) cathode catalysts.

might have resulted from different ORR paths reflecting different MEA components. The first arc corresponding to the higher frequency region exhibited the mass-diffusion phenomenon in the ORR of the anode catalyst layer, whereas the second arc corresponding to the lower frequency region exhibited the mass-diffusion phenomenon observed in the ORR of the other components, such as the catalyst coated on the MPL [27]. The double arcs both became larger or even diverged, which indicated that the diffusion problem began to hinder mass transport during long-term operation. Fig. 7(c) plots the CTR spectrum of the individual cathode. The arc also became larger but was not divergent, and the increase was relatively smaller on the cathode side than on the anode side. Thus, the results might exhibit that the diffusion was less problematic on the cathode side than on the anode side. Fig. 7(d) plots the EIS spectrum of the individual membrane. Since the EIS spectra were similar, the membrane was not the dominant influence on cell performance.

Fig. 8 shows the CV testing results obtained by the hydrogen-desorption method, and the individual results in the anode and cathode catalysts are shown, respectively, in Fig. 8(a) and (b). The ECA loss estimated not only the microstructural change, such as catalyst agglomeration and growth, but also the chemical degradation caused by the poisoning of the catalysts. After 1450 h test from Fig. 5, the ECA values of MEA listed in Table 1 decreased 46.1% and 39.9% in the anode and cathode catalysts, respectively. Notably, with the proposed strategies for optimizing cathode conditions, the ECA loss was greater in the anode catalyst; these results are opposite to our previous work [7]. Regarding the HFR of the full-cell impedance spectrum, the cause of increased resistance was revealed after removing the MEA from the test block. Surprisingly, a thin metal oxide was found on the surface of the test block, even though SS Type 316 material was used. The phenomenon was more serious on the cathode side. Therefore, the cell was examined after polishing the test block to evaluate the actual MEA performance loss. Fig. 9(a) shows polarization curves before and after 1450 h test from Fig. 5. The peak performance increased about 8.2% after polishing the test block. Fig. 9(b) and (c) shows the ECA results in the anode and cathode catalysts, respectively. The ECA loss in the anode catalyst was 38% after polishing the test block, while that in the cathode catalyst was only 25.6%. Thus, the actual ECA losses due to formation of a metal oxide on the surface of the SS Type 316 were estimated at 8.1% and 14.3% on the anode and cathode sides, respectively.

4. Conclusions

The proposed strategies for optimizing the cathode condition were carried out to improve the durability of a Direct Methanol Fuel Cell. By means of regulating the air on/off condition during the load-off mode and the load on/off interval and moderate air flow rate during the load-on mode, the degradation could be further suppressed, especially on the cathode side. Nevertheless, the cell performance was degraded by about 50–60% after 1450 h test from Fig. 5, and the dominant factor affecting the cell performance was clarified by the polarization curves, EIS measurements and ECA results. The $|\Delta V/\Delta I|$ value associated with the resistance R was used to identify the greatest effects on performance, and the anode was found to be the major detrimental component. By incorporating EIS measurements, the performance loss of the MEA could be explained in detail. Thus, the mass-diffusion problems, including the CO_2 elimination and methanol transportation caused by microstructural changes to the MPL on the anode side, were considered the degradation mechanisms. The ECA results indicated, impressively, the ECA loss in the cathode catalyst was relatively lower than that in the anode catalyst, which implied the useful effort of the proposed strategy for optimizing cathode operating conditions. The loss in the cathode catalyst was relatively lower than that in the anode catalyst. Besides, a thin metal oxide was discovered on the surface of the test block after 1450 h test from Fig. 5. However, the actual performance loss of the MEA could be obtained by erasing the impact of the metal oxide.

References

[1] B. McNicol, D. Rand, K. Williams, J. Power Sources 83 (1999) 5.
[2] K.B. Prater, J. Power Sources 61 (1996) 105.

[3] J. Prabhuram, N.N. Krishnan, B. Choi, T.H. Lim, H.Y. Ha, S.K. Kim, Int. J. Hydrogen Energy 35 (2010) 6924.
[4] U.B. Demirci, J. Power Sources 169 (2007) 239.
[5] E. Antolini, J.R.C. Salgado, E.R. Gonzalez, Appl. Catal., B 63 (2006) 137.
[6] K. Sundmacher, T. Schultz, S. Zhou, K. Schott, M. Ginkel, E.D. Gilles, Chem. Eng. Sci. 5 (2001) 333.
[7] H.C. Cha, C.Y. Chen, J.Y. Shiu, J. Power Sources 192 (2009) 451.
[8] M. Fowler, J.C. Amphlett, R.F. Mann, B.A. Peppley, P.R. Roberge, J. New Mater. Electrochem. Syst. 5 (2002) 255.
[9] W. Schmittinger, A. Vahidi, J. Power Sources 180 (2008) 1.
[10] J.K. Lee, J. Choi, S.J. Kang, J.M. Lee, Y. Tak, J. Lee, Electrochim. Acta 52 (2007) 2272.
[11] H. Kima, S.J. Shin, Y.G. Park, J. Song, H.T. Kim, J. Power Sources 160 (2006) 440.
[12] C.Y. Chen, P. Yang, Y.S. Lee, K.F. Lin, J. Power Sources 141 (2005) 24.
[13] C.Y. Chen, J.Y. Shiu, Y.S. Lee, J. Power Sources 159 (2006) 1042.
[14] X. Wang, J.M. Hu, I.M. Hsing, J. Electroanal. Chem. 562 (2004) 73.
[15] K.T. Jeng, C.C. Chien, N.Y. Hsu, W.M. Huang, S.D. Chiou, S.H. Lin, J. Power Sources 164 (2007) 33.
[16] C.Y. Du, T.S. Zhao, C. Xu, J. Power Sources 167 (2007) 265.
[17] J.S. Lee, K.I. Han, S.O. Park, H.N. Kim, H. Kim, Electrochim. Acta 50 (2004) 807.
[18] H.C. Cha, C.Y. Chen, R.X. Wang, C.L. Chang, J. Power Sources 196 (2011) 2650.
[19] S.H. Yang, C.Y. Chen, W.J. Wang, J. Power Sources 195 (2010) 2319.
[20] S.H. Uhm, S.T. Chung, J.Y. Lee, J. Power Sources 178 (2008) 34.
[21] P. Piela, T.E. Springer, J. Davey, P. Zelenay, J. Phys. Chem. C 111 (2007) 6512.
[22] T.R. Ralph, G.A. Hards, J.E. Keating, S.A. Campbell, D.P. Wilkinson, M. Davis, J. St-Pierre, M.C. Johnson, J. Electrochem. Soc. 144 (1997) 3845.
[23] J.Y. Park, M.A. Scibioh, S.K. Kim, H.J. Kim, I.H. Oh, T.G. Lee, H.Y. Ha, Int. J. Hydrogen Energy 34 (2009) 2043.
[24] U.A. Paulus, T.J. Schmidt, H.A. Gasteiger, R.J. Behm, J. Electroanal. Chem. 495 (2001) 134.
[25] Y. Shao, G. Yin, Y. Gao, P. Shi, J. Electrochem. Soc. 153 (2006) A1093.
[26] C. Eickes, P. Piela, J. Davey, P. Zelenay, J. Electrochem. Soc. 153 (2006) A171.
[27] S.H. Yang, C.Y. Chen, W.J. Wang, J. Power Sources 195 (2010) 3536.